Developmental Cell
Article

Dll4 and PDGF-BB Convert Committed Skeletal Myoblasts to Pericytes without Erasing Their Myogenic Memory

Ornella Cappellari,[1,2,3] Sara Benedetti,[1,3] Anna Innocenzi,[3] Francesco Saverio Tedesco,[1,3] Artal Moreno-Fortuny,[1] Gonzalo Ugarte,[3,6] Maria Grazia Lampugnani,[4] Graziella Messina,[5] and Giulio Cossu[1,3,5,*]
[1]Department of Cell and Developmental Biology and Centre for Stem Cells and Regenerative Medicine, University College London, WC1E 6DE London, UK
[2]Department of Anatomy, Histology, Forensic Medicine, and Orthopedics, "Sapienza" University of Rome, 00161 Rome, Italy
[3]Division of Regenerative Medicine Stem Cells and Gene Therapy, San Raffaele Hospital, 20132 Milan, Italy
[4]IFOM, The FIRC Institute of Molecular Oncology Foundation, 20139 Milan, Italy
[5]Department of Biosciences, University of Milan, 20129 Milan, Italy
[6]Present address: Departamento de Quimica y Biologia, Universidad de Santiago de Chile, 9160000 Santiago, Chile
*Correspondence: g.cossu@ucl.ac.uk
http://dx.doi.org/10.1016/j.devcel.2013.01.022

SUMMARY

Pericytes are endothelial-associated cells that contribute to vessel wall. Here, we report that pericytes may derive from direct conversion of committed skeletal myoblasts. When exposed to Dll4 and PDGF-BB, but not Dll1, skeletal myoblasts downregulate myogenic genes, except Myf5, and upregulate pericyte markers, whereas inhibition of Notch signaling restores myogenesis. Moreover, when cocultured with endothelial cells, skeletal myoblasts, previously treated with Dll4 and PDGF-BB, adopt a perithelial position stabilizing newly formed vessel-like networks in vitro and in vivo. In a transgenic mouse model in which cells expressing MyoD activate Notch, skeletal myogenesis is abolished and pericyte genes are activated. Even if overexpressed, Myf5 does not trigger myogenesis because Notch induces Id3, partially sequestering Myf5 and inhibiting MEF2 expression. Myf5-expressing cells adopt a perithelial position, as occasionally also observed in wild-type (WT) embryos. These data indicate that endothelium, via Dll4 and PDGF-BB, induces a fate switch in adjacent skeletal myoblasts.

INTRODUCTION

Cells of the dorsal somites are committed to skeletal myogenesis by signals such as Wnt and Shh that emanate from neighboring tissues (Cossu and Borello, 1999). Some committed cells promptly differentiate to form the myotome, whereas other progenitors, marked by the expression of Pax3 and Pax7, proliferate giving rise to all subsequent populations of embryonic, fetal, and postnatal myogenic cells that differentiate at specific stages of development (Buckingham and Relaix, 2007). It is still unknown how proliferation and differentiation are asynchronously regulated during development (Biressi et al., 2007a). However, it is generally assumed that, once committed, skeletal myoblasts are fated to differentiate into myofibers after variable rounds of cell divisions. Indeed, highly purified embryonic or fetal myoblasts, once explanted in culture, readily differentiate into oligo or multinucleated myotubes (respectively) and do not require any instructive signal (Biressi et al., 2007b), thus indicating that they are already committed to myogenesis. Moreover, embryonic myoblasts are resistant to the action of molecules such as TGF-β and BMP that rather inhibit myogenesis in later populations of myogenic cells such as fetal myoblasts. However, it was previously demonstrated that the Notch pathway inhibition (through Dll1 gene ablation) in the embryo leads to a premature myogenic differentiation and depletion of the muscle progenitor population (Schuster-Gossler et al., 2007). Conversely, overexpression of Dll1 inhibits MyoD-mediated myogenesis but does not affect Pax3 or Myf5 expression (Delfini et al., 2000). Thus, it appears that only Notch activation inhibits embryonic myogenesis. Interestingly, the Notch ligands Dll1 and Dll4 are expressed by developing endothelium (Kume, 2012) together with PDGF-BB, which recruits pericytes from the surrounding mesenchyme (Hellström et al., 1999). These data raised the possibility that those myogenic progenitors that are in close proximity to the developing endothelium in embryonic and fetal skeletal muscle may be prevented from progressing toward terminal myogenesis and converted to a perithelial fate via Notch ligands and PGDF-BB. By a combination of in vitro and in vivo approaches, we show that this is indeed the case, thus demonstrating that a fate switch may occur as a natural developmental process.

RESULTS

Dll4 and PDGF-BB Inhibit Skeletal Myogenesis and Induce Pericyte Markers in Pax3-Expressing Skeletal Myoblasts

Embryonic myoblasts, sorted from Pax3$^{GFP/+}$ E11.5 embryos (Figures S1A and S1B available online) after removal of neural tube and dorsal root ganglia, were cultured in standard conditions (see Experimental Procedures). All of the cells expressed

GFP (Figure S1D, right panel), and virtually all (>95%) underwent myogenic differentiation, generating thin oligonucleated, MyHC-expressing myotubes (Figure 1A, upper panel). To rule out possible contamination by neural cells, immunofluorescence with an antibody against Sox2 was performed on Pax3$^{GFP/+}$ cells, digested from the whole embryo (Figure S1E, upper panel) or on Pax3$^{GFP/+}$ cells digested from embryos whose neural structures had been previously removed (Figure S1E, lower panel). Sox2-expressing cells were easily detected in the preparation from the whole embryo but were completely absent in the preparation from aneural embryos. As previously shown for Myf5$^{GFP/+}$ embryonic myoblasts (Biressi et al., 2007b), Pax3$^{GFP/+}$ cells were also found to be insensitive to many molecules such as BMP, bFGF, and TGF-β (Figure S1C), which are known to inhibit fetal myogenesis. However, when Pax3$^{GFP/+}$ myoblasts were cocultured with human umbilical vein endothelial cells (HUVECs), some cells (approximately 10% of the population) were found to express alkaline phosphatase (AP), a pericyte marker (Figure S1E, lower-right panel). Because it is known that endothelial cells are able to recruit pericytes and produce Notch ligands and PDGF-BB (Scehnet et al., 2007; Hellström et al., 1999), we cultured Pax3$^{GFP/+}$ myoblasts in dishes coated with the Notch ligand Dll4 in the presence of PDGF-BB. Under these conditions, skeletal myogenesis was almost completely (<5% of MyHC+ cells) inhibited (Figure 1B, upper panel, and Figure 1F). Within 12 hr, Dll4 and PDGF-BB induced expression of pericyte markers such as AP, RGS5, and NG2, which were practically undetectable in nontreated control cells by quantitative PCR (qPCR) (Figure 1F), immunofluorescence (with the exception of rare NG2$^+$ cells in control cells: Figures 1B–1D, middle panel, and 1F), or western blot analysis (Figure 1E). Among other pericyte markers, PDGF receptor β (PDGF-Rβ) transcript (mRNA), which is also expressed in myoblasts, was upregulated 2-fold after exposure to Dll4 and PDGF-BB (Figure 1F). Both qPCR and western blot analysis revealed an enhanced expression of Myf5, at variance with all the other myogenic markers tested, which were strongly downregulated (Figures 1E and 1F). Exposure to Dll4 and PDGF-BB did not interfere with the low level of apoptosis usually observed in embryonic myoblasts (<5%; data not shown). However, treated cells, at variance with control cells, continued to proliferate (Figure S1G). Dll4 and PDGF-BB-dependent inhibition of myogenesis was found to be irreversible after subculture in fresh, control medium. In contrast, the block of Notch signaling with L-685,458, a γ-secretase inhibitor (that hampers proteolytic activation of Notch receptors, thus preventing nuclear translocation of its intracellular domain) (De Strooper et al., 1999) in Pax3$^{GFP/+}$ Dll4 and PDGF-BB-treated cells, led to a rapid and massive (>80%) myogenic differentiation (Figures 1A–1D, lower panel, and 1F) and silencing of pericyte genes (Figures 1B and 1C, lower panel, 1F). When compared with bona fide NG2$^+$/PECAM$^-$ pericytes sorted from wild-type (WT) aneural embryos, Pax3^{GFP+} myoblasts, exposed to Dll4 and PDGF-BB, were found to express comparable and in some cases even higher levels of the pericyte markers analyzed (Figure 1G). All the experiments described above were conducted by exposing cells to Dll4 and PDGF-BB, and L-685,458 for the phenotype reversion. In order to test the role of each of these factors, we repeated the experiment using the two molecules separately or in combination. Figures S2A–S2D show that PDGF-BB alone did not induce AP expression but potentiated its activation when administered together with Dll4 that was active also when administered alone. To test the specificity of Dll4, we repeated the same experiment using other Notch activators such as Dll1 and Jagged1. As expected, Pax3$^{GFP/+}$-expressing myoblasts did not differentiate in the presence of Dll1 and Jagged1. However, under these conditions, treated cells did not activate expression of pericyte markers (Figures S2E and S2F), indicating that the observed effect is specific for Dll4 and not redundant among the other Notch ligands tested. In order to test whether Dll4 exerts this effect on every mesoderm cell type, we similarly treated 10T$^{1/2}$ fibroblasts. qPCR (Figure S3B) and immunostaining for AP (Figure S3A) revealed no activation of pericyte markers in fibroblasts exposed to Notch ligand Dll4 and PDGF-BB, indicating that recruitment to a pericyte fate, though probably shared by other cell types, is not an unspecific response of any cell to Dll4 and PDGF-BB.

Dll4 and PDGF-BB-Treated Myoblasts Associate with Endothelial Cells to Form Vessel-like Networks In Vitro and In Vivo

We then tested the ability of myoblasts exposed to Dll4 and PDGF-BB to form vessel-like structures in vitro and in vivo. HUVECs cultured alone in Matrigel usually form an unstable network that disappears after a few days (Nakatsu et al., 2003). In contrast, when we sorted bona fide pericytes (NG2$^+$/PECAM) from aneural GFP$^+$ mouse embryos and combined them with HUVECs in an in vitro Matrigel sandwich, they formed vessel-like networks that were stable for many days. Virtually all GFP$^+$ cells were closely associated with HUVECs assuming a clear perithelial position (Figures 2A–2C and S4G–S4J). The same approach was repeated with untreated Pax3$^{GFP/+}$ cells, some of which initially (within the first 12 hr) associated to the HUVEC endothelial network (Figures S4A–S4C) and assumed a perithelial position; however, after additional 24 hr, the majority of the population rapidly differentiated into thin oligonucleated myotubes, indicating that they undergo skeletal myogenesis also under this experimental condition (Figures 2D–2F) and contribute to the disassembly of the endothelial network that had formed after 12 hr (Figures S4A–S4C). Only when Pax3$^{GFP/+}$ cells had been previously treated with Dll4 and PDGF-BB and cultured in Matrigel together with HUVECs (identified in Figures 2H, 2I, 2K, 2L, and 2N, by BV9 human-specific anti-VE-cadherin in red), they closely associated to them in a perithelial position and formed a vessel-like network that remained stable for up to 2 weeks (Figures 2J–2L and S4D–S4F). The same effect was observed when a Matrigel plug was implanted subcutaneously into nude mice: after 2 weeks, a large vessel network, connected with the host vasculature, had developed (Figure 2M). Immunofluorescence analysis confirmed close association of Dll4 and PDGF-BB-treated, Pax3$^{GFP/+}$ myoblasts with HUVECs labeled by an anti-BV9 antibody (Figure 2N), thus demonstrating that the vessel-like structures formed in the Matrigel plug consist of both endothelium and myoblast-derived pericytes, that contribute to network stability. To confirm that HUVEC-derived Dll4 was responsible for pericyte recruitment, we silenced in vitro Dll4 expression, testing four specific shRNAs and selecting the most efficient (shRNA4) for in vivo experiments (Figures S5A and S5B). Under these conditions, HUVECs were no longer

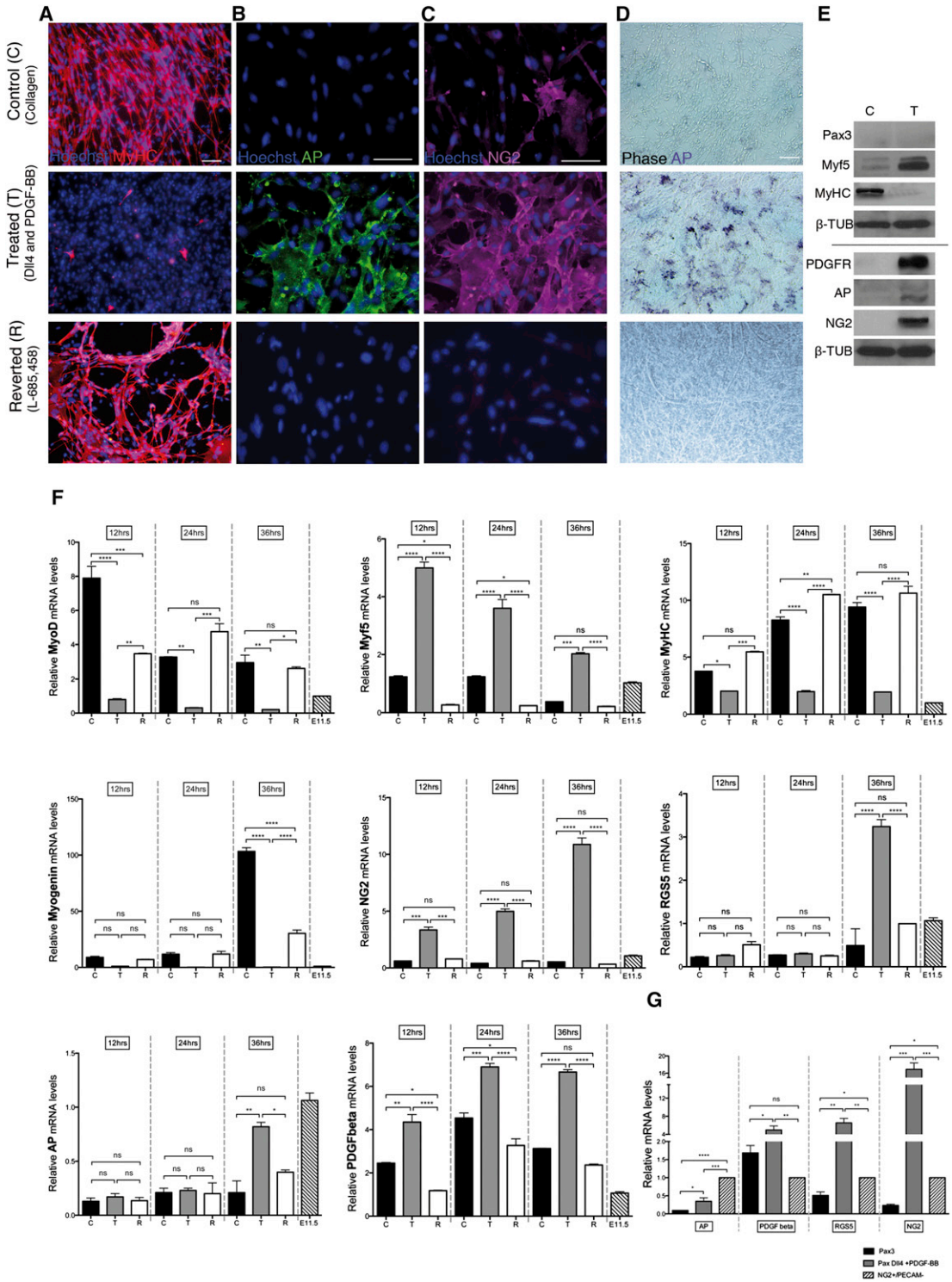

Figure 1. Dll4 and PDGF-BB Inhibit Skeletal Myogenesis and Induce Pericyte Markers

(A–C) Immunofluorescence analysis of markers expressed by purified Pax3$^{GFP/+}$ embryonic myoblasts (E11.5) in control culture condition (Control, A–C, upper panel) and after treatment with Dll4 and PDGF-BB (Treated, A–C, middle panel) and of treated cells after exposure to γ-secretase inhibitor (L-685,458), a Notch inhibitor (Reverted, A–C, lower panel). Cells were stained with a anti-MyHC (red), AP (green), NG2 (violet) antibodies, and Hoechst (blue). Scale bars, 100 μm (B and C) and 50 μm (A).

(D) Phase-contrast analysis of AP reaction (violet) of control (upper panel), treated (middle panel), and reverted cells (lower panel). Scale bar, 50 μm.

(E) Western blot analysis of myogenic (Pax3, Myf5, MyHC) and pericyte (PDGF-R, NG2, AP) markers expressed by control (C) and treated (T) cells. β-Tubulin (β-TUB) was chosen as a normalizer.

(legend continued on next page)

able to consistently recruit pericytes, though few cells still associated to them in an unstable network visible at 12 hr (Figures S4K and S4L) but were no longer present at later times. As a matter of fact, 2 weeks after the implant into a nude mouse of a Matrigel plug of shRNADll4HUVECs and Dll4 and PDGF-BB-treated Pax3^{GFP+} cells, there was no detectable vessel formation inside the plug (Figure S5B).

Dll4 and PDGF-BB Also Convert Myf5-Expressing Myogenic Cells

Although Pax3 expression marks skeletal muscle commitment in the embryo, cells entering the myogenic differentiation pathway activate bHLH such as *Myf5* and/or *Myod* (Buckingham and Relaix, 2007). Therefore, we investigated whether Dll4 and PDGF-BB might also convert Myf5-expressing cells that have progressed toward myogenic differentiation more than Pax3^{+} cells. To this aim, we sorted Myf5$^{GFP/+}$ embryonic (E11.5) and fetal (E16.5) myoblasts, from the Myf5$^{GFP/+}$ transgenic mouse by FACS (Figure 3A). Under the same experimental conditions previously employed for Pax3$^{GFP/+}$-expressing myoblasts, both embryonic (Figure 3A, left columns) and fetal (Figure 3B, left columns) Myf5$^{GFP/+}$-expressing myoblasts were no longer able to differentiate into skeletal myotubes and activated expression of AP (right columns of both Figures 3A and 3B). qPCR revealed that pericyte genes were activated in both myoblast populations, although not all at the same extent than in Pax3$^{GFP/+}$ myoblasts: as an example, RGS5 was much more robustly upregulated in fetal myoblasts only, whereas increase in NG2 expression was modest in both Myf5$^{GFP/+}$ populations (Figure 3C). This suggests that cells at a more advanced stage of the myogenic differentiation pathway can still be converted to a pericyte fate.

Committed Skeletal Myoblasts Can Be Converted to Pericytes during In Vivo Development in a Transgenic Mouse Model

Rosa^{NICD} transgenic mice (Murtaugh et al., 2003) express the Notch intracellular domain (NICD) and thus activate the Notch pathway after Cre recombination. To mimic the same condition we had created in vitro, we crossed Rosa^{NICD} with MyoD^{iCRE} mice (Kanisicak et al., 2009) so that only cells that express MyoD also activate Notch. Although it is well known that Notch inhibits in vitro myogenesis (Kopan et al., 1994), we investigated whether Notch activation would induce also in vivo a fate switch of myoblasts toward a pericyte phenotype. As expected, E9.5 double-transgenic embryos appeared similar to WT embryos (data not shown), consistent with the notion that the early myotome is formed under the transcriptional control of Myf5, before MyoD activation (Cossu et al., 1996). On the other hand, at E11.5, MyoD^{iCRE}:ROSA^{NICD} mutant embryos appeared to be smaller compared to WT and showed a modest edema (Figure 4A). At this stage of development, expression of myogenic markers (black bars in quantitative real-time PCR panel, Figure 4B) MyHC and MyoD appeared slightly reduced (though differences were not statistically significant), whereas there were no significant variations of pericyte marker expression (white bars in qPCR panel, Figure 4B) with the exception of a modest upregulation of AP (Figure 4B). Also, western blot analysis did not show major differences (Figure 4C) between the WT and MyoD^{iCRE}:ROSA^{NICD} mutant embryos. At the histological level, no major differences were observed (Figure 4D, top images), but immunofluorescence analysis revealed a reduced number of MyHC-expressing cells in the proximal region of the limbs (arrows in Figure 4D, bottom images), although the myotomes appeared to be similar. At this stage, too few cells have terminally differentiated in order to detect MyHC by western blot analysis in extracts of total embryos (Figure 4C).

Immunofluorescence analysis at a higher magnification of trunk mesoderm revealed many cells expressing Myf5 and smooth α actin (SMA; a protein expressed at this stage both in smooth and skeletal myoblasts; Babai et al., 1990; Herman and D'Amore, 1985) in both WT and MyoD^{iCRE}:ROSA^{NICD} embryos (Figure 4E, bottom images); on the contrary, widespread expression of AP was only detected in MyoD^{iCRE}:ROSA^{NICD} embryos, and not in WT (Figure 4E, top images), where it usually appears only around small vessels at E13.5 (unpublished data). At E13.5, the abnormal phenotype was more evident in mutant embryos (Figure 4F). Histological analysis did not reveal major differences (Figure 4I, top images). On the other hand, differences in gene and protein expression were now remarkable and statistically significant (Figures 4G and 4H); MyHC+ fibers appeared to be strongly reduced in the mutant embryo (Figure 4I, bottom images). Confocal microscopy confirmed a close association of cells coexpressing Myf5 and AP, with the endothelium of medium- and small-size vessels (Figure 4J, arrow in upper panel). At E16.5, mutant fetuses were severely compromised showing a prominent edema (Figure 5A) and a dramatically reduced skeletal muscle differentiation (Figure 5D) confirmed by qPCR (Figure 5B) and western blot (Figure 5C) analyses. Similarly to what was observed in vitro, Myf5 expression appeared increased by 3-fold (Figure 5B) and was clearly detected by immunofluorescence, whereas it appeared fainter in WT embryos where expression is known to decrease at this stage of development (Ott et al., 1991). Mutant embryos also overexpressed other pericyte markers such as the PDGF-Rβ that we found to be sometimes coexpressed with AP in immunofluorescence analyses (Figures S6C and S6D). Dll4 expression was markedly increased in mutant fetuses being localized in vessels and also, at a very high level, in mononucleated cells not associated to vessels (Figure S6E), only few of which

(F) Quantitative real-time PCR analysis of relative mRNA expression of MyoD, Myf5, MyHC, myogenin, NG2, RGS5, AP, and PDGF-R β in control cells (C, black bars), treated cells (T, gray bars), and in cells treated for the same time with Dll4 and PDGF-BB and then with L-685458 (R, white bars). Cells were analyzed at different time points (12, 24, and 36 hr) of culture. Cells treated additionally with Notch inhibitor (L-685,458) were treated with the inhibitor for the same time they had been treated with the Dll4 and PDGF-BB, i.e. 12, 24, and 36 hr more after Notch activation (thus 24, 48, and 72 hr in total after). Data are expressed as mean ± SEM.

(G) Quantitative real-time PCR performed on bona fide pericytes versus converted myoblasts. Results show that sorted pericytes (NG2^{+}/PECAM^{-} population) express the same markers as converted myoblasts, although converted myoblasts express pericyte markers at higher levels than bona fide pericytes.

*$p < 0.05$, **$p < 0.005$, ***$p < 0.0005$, ****$p < 0.00005$, one-way ANOVA, ns, not significant. See also Figures S1–S3.

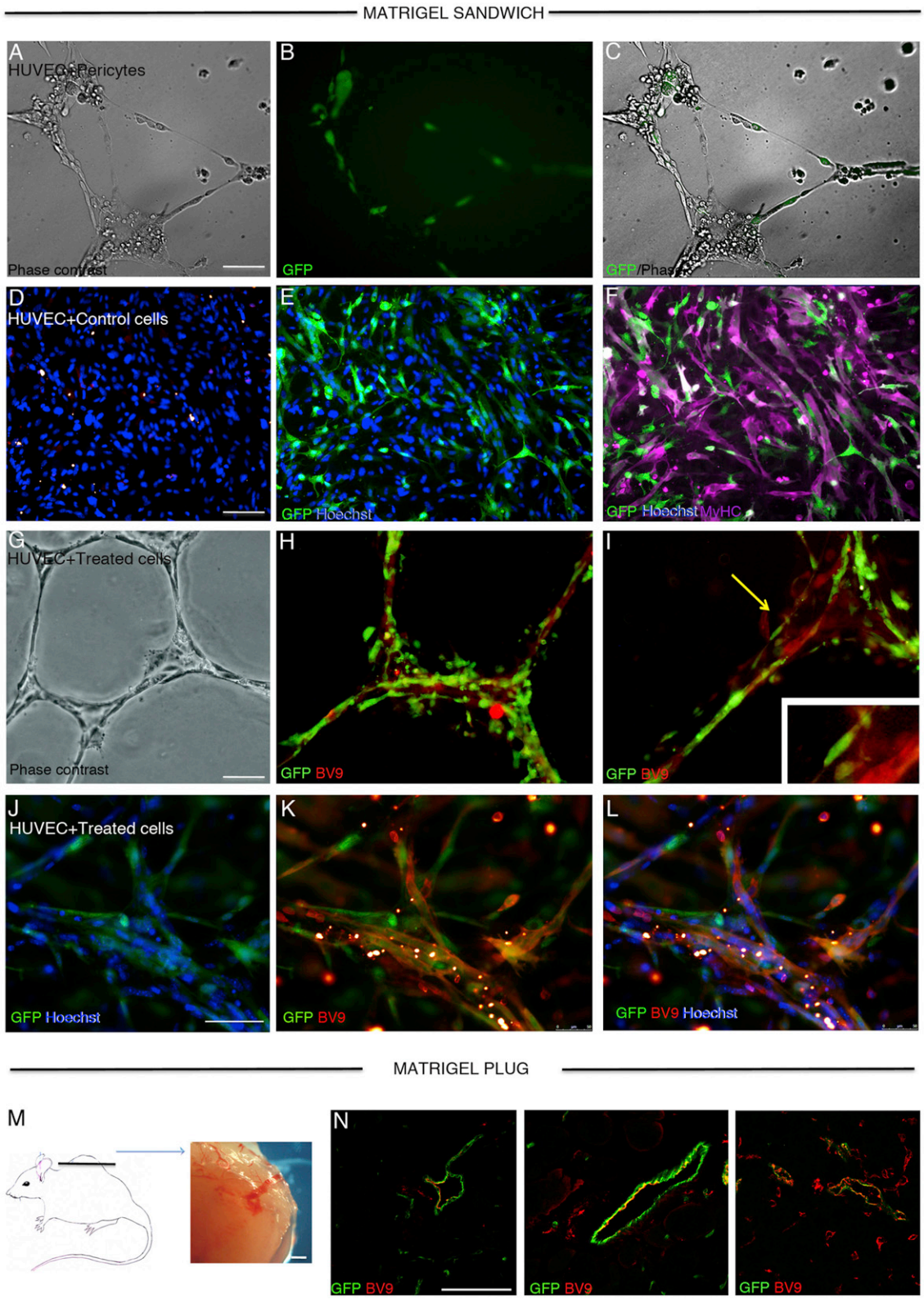

Figure 2. Angiogenesis Assay In Vitro and In Vivo

(A–C) In vitro Matrigel sandwich (in vitro assay) containing a mixture of HUVECs and bona fide pericytes NG2^{+}/PECAM^{-} sorted from Homo-GFP (Hadjantonakis et al., 1998) E11.5 mouse embryos. (A) Phase contrast of HUVECs mixed with pericyte control cells. (B and C) HUVECs mixed with pericyte GFP^{+} stained with anti-GFP antibody (green).

(legend continued on next page)

expressed Myf5 (Figures S6A and S6B). The nature of these cells remains to be investigated.

From E16.5 to E18.5, alterations in development were exacerbated in the mutant embryo, lung formation was compromised, and the edema became even more severe (Figure 5F). Newborn mice were smaller, edematous, less vascularized, and did not breathe. They died immediately after birth. A similar phenotype has been reported for the Myf5/MyoD double-mutant embryos (Rudnicki et al., 1993). Histological and immunofluorescence analysis revealed dramatic differences in skeletal muscle formation with few residual muscle fibers in the mutant fetus (Figure 5I). Myf5 expression remains at very high levels (Figures 5G and 5H), whereas, as mentioned, it decreases further in WT fetuses; similarly, pericyte markers were expressed at high levels (Figures 5G and 5H). Moreover, we observed a high number of Myf5-expressing cells closely associated to vessels (Figure 5J, right panel). These results confirm that Notch activation in myogenic cells is able, also in vivo, to suppress myogenesis and activate the expression of pericyte genes, very often in Myf5-expressing cells.

Direct Conversion of Myoblast to Pericytes Also Occurs at Low Frequency in WT Embryos

The phenotype described above reflects an abnormal activation of Notch in myogenic progenitors in vivo. We wondered whether Notch activation might enhance a phenomenon of fate shift that may infrequently occur during normal embryogenesis, especially in those cells at the border of two different anlagen and thus exposed to similar concentrations of signals dictating different fates (Bianco and Cossu, 1999). To test this possibility, we examined WT fetuses at E16.5 using different immunofluorescence probes. Figures 6A–6C show a longitudinal section of a blood vessel (identified by staining with SMA; green in Figure 6A) where a single Myf5-expressing nucleus (red in Figure 6B) was clearly detected. Figure 6D shows a transversal section of a medium-size vessel, double stained for the endothelial marker PECAM (red) and the pericyte marker NG2 (magenta) where two Myf5-expressing cells (arrows pointing to green nuclei) were clearly detected in a perithelial position, within the vessel wall. Moreover, by crossing MyoD^{iCRE} mice with Rosa-LacZ floxed (Figure 6E) or Rosa^{EYFP} (Figures 6F–6H), we could detect at a low frequency (i.e., one example per five 20× microscopic fields) areas where LacZ or GFP-expressing cells (hence, derived from MyoD-expressing progenitors) were clearly detected inside the vessel wall (arrows in Figures 6E, 6G, and 6H) even though not all the nuclei had adopted the typical elongated pericyte morphology. Low magnification (Figure 6F) shows that immunofluorescence labeling was correct and that the large majority of endothelial cells (red) were intermixed with myogenic cells as expected. Moreover, in MyoD^{iCRE}:Rosa^{EYFP} mice, we could detect several YFP^{+} cells surrounding the endothelial layer of a medium-size artery, within the NG2^{+} cells (Figures 6I and 6J). At a higher magnification (Figures 6K and S7), confocal analysis revealed several Myf5-expressing cells (arrows) also expressing AP (identified by a red fluorescent substrate) Together, these data indicate that skeletal myoblasts may occasionally adopt a pericyte fate also during normal embryogenesis.

Notch-Induced ID3 and MEF2 Inhibit Myf5 and Its Ability to Activate Myogenesis

Dll4 expression in vitro and NICD activation in vivo upregulate Notch3 and Notch1 expression that, in myogenic cells, leads to a strong downregulation of myogenic markers such as MyoD (one well-known Notch target) and Myosin expression (Kopan et al., 1994). Unexpectedly, Myf5 expression was robustly upregulated, possibly as an attempt to compensate for the absence of MyoD. However, despite its high level of expression (Figures 1, 3, 4, and 5), Myf5 was not sufficient to drive terminal myogenic differentiation (see above). By qPCR, we first confirmed (Langlands et al., 1997) that in response to Dll4 and PDGF-BB, also Pax3$^{GFP/+}$ myoblasts upregulate the expression of Id3, Notch3, Twist, and Lunatic Fringe (Figures 7A–7D). Thus, it is possible that Notch-induced upregulation of Id3 and Twist may interfere with Myf5 activity (Langlands et al., 1997). Indeed, Myf5 protein forms a complex with Id3 (the most upregulated member of the Id family after Notch activation) and, thus, may become unable to bind the myogenin promoter and trigger myogenesis. Therefore, coimmunoprecipitation was performed in E16.5 WT embryos and E16.5 MyoD^{iCRE}:ROSA^{NICD}, which revealed binding of the two proteins Myf5 and Id3, thus providing one possible explanation for the inability of Myf5 to activate myogenesis (Figure 7F). Nevertheless, a ChIP analysis revealed that Myf5 was still able to bind to the myogenin promoter, most likely because the Id3 sequestration of Myf5 was only partial, given its overexpression (Figure 7E). On the other hand, MEF2 was correctly expressed in WT embryos but undetectable in mutant embryos (Figure 7G) as already reported by Wilson-Rawls et al. (1999), and therefore, even if Myf5 is partially able to bind the myogenin promoter, the

(D–F) In (D), Hoechst staining of HUVECs mixed with untreated Pax3^{GFP+} embryonic myoblasts. It is possible to detect white dots that represent Lam A/C-positive human nuclei. In (E), cells are stained with anti-GFP antibody (green) that marks sorted Pax3$^{GFP/+}$ myoblasts. In (F), cells are stained also with anti-MyHC antibody (violet) that marks differentiated embryonic myotubes. This culture lasts between 12 and 24 hr, then myogenic cells differentiate.

(G–I) Matrigel sandwich containing Pax3$^{GFP/+}$ cells, previously treated with Dll4 and PDGF-BB then mixed with HUVECs. Inset shows higher magnification of the area indicated by the arrow. Phase-contrast analysis (G) shows a stable endothelial network, which has been stained (H and I) with human-specific anti-VE-cadherin BV9 antibody (red) to stain HUVECs and with anti-GFP antibody (green) that stains Pax3$^{GFP/+}$ cells. Inset shows higher magnification of the area identified by the arrow.

(J–L) Immunofluorescence of a 2 week stable endothelial network in a Matrigel sandwich containing Pax3$^{GFP/+}$ cells, previously treated with Dll4 and PDGF-BB then mixed with HUVECs. Cells were labeled with Hoechst (blue), GFP (green), and anti-BV9 (red) antibodies.

(M) Scheme of an in vivo Matrigel plug: a mixture of Dll4-PDGFBB treated Pax3$^{GFP/+}$ cells plus HUVECs embedded into Matrigel has been implanted subcutaneously into nude mice. (right panel) The right image shows gross anatomy of freshly removed Matrigel plug, 2 weeks after implantation.

(N) Confocal analysis of representative cryostat sections of the Matrigel plug containing a mixture of Dll4 and PDGF-BB-treated Pax3$^{GFP/+}$ and HUVECs: Pax3$^{GFP/+}$ cells are stained with anti-GFP (green), whereas HUVECs for BV9 (red).

Scale bars, 50 μm. See also Figures S4 and S5.

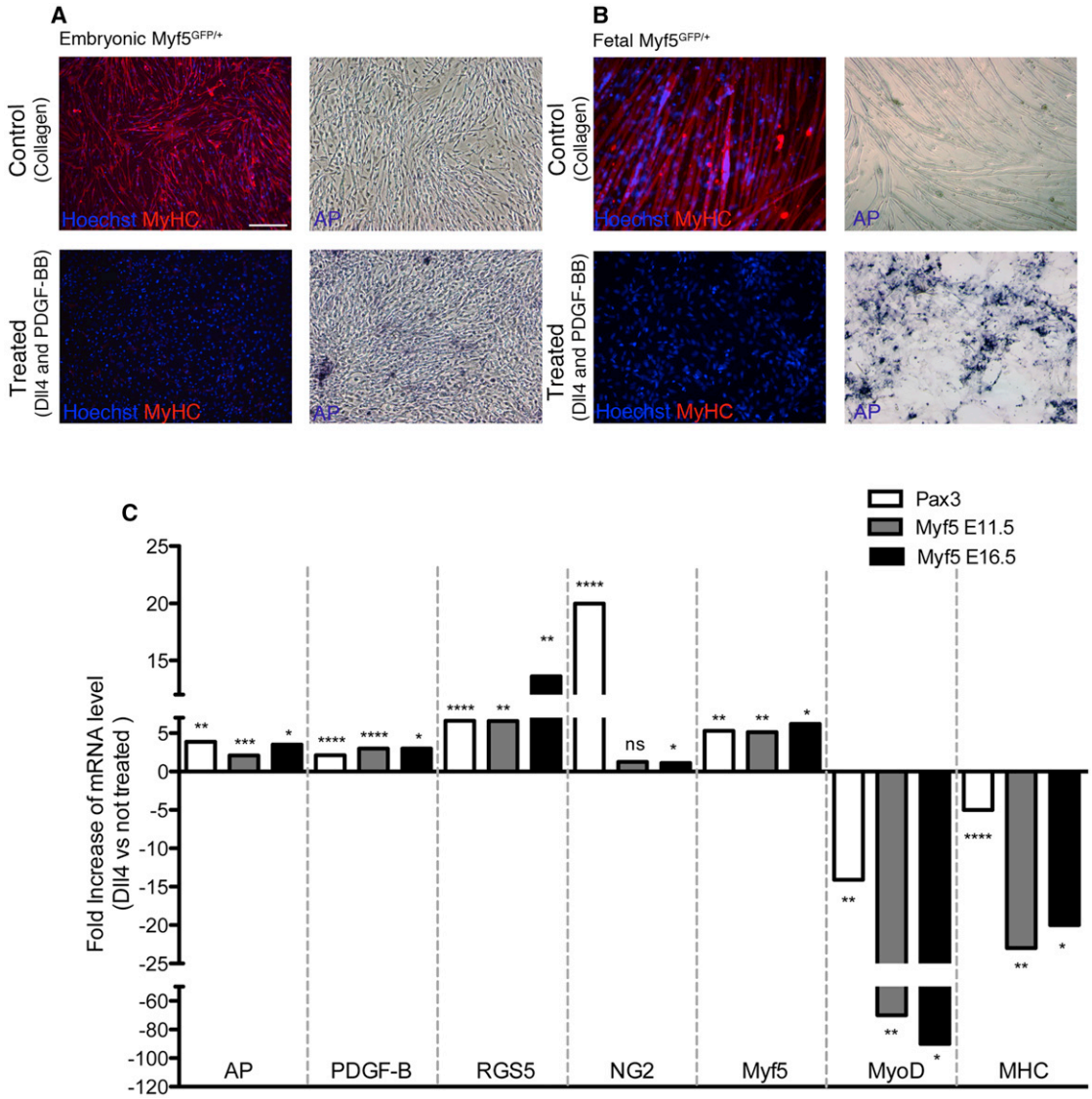

Figure 3. Dll4 and PDGF-BB Inhibit Fetal Skeletal Myogenesis and Also Induce Pericyte Markers

(A) Immunofluorescence analysis of embryonic Myf5^{GFP+}. Differentiated cells are stained with anti-MyHC antibody (red) and Hoechst (blue). As described above for the Pax3$^{GFP/+}$ cells, sorted Myf5$^{GFP/+}$ plated on Dll4 and PDGF-BB (Treated) do not differentiate (left column) and express Alkaline Phosphatase (right column).

(B) Immunofluorescence analysis on fetal Myf5$^{GFP/+}$. Differentiated cells are stained with MyHC (red) and Hoechst (blue). Inhibition of fetal myogenesis is almost total and after exposure to Dll4 and PDGF-BB (left column) they express Alkaline Phosphatase at high level (right column).

(C) Quantitative real-time PCR analysis of myogenic (MyoD, Myf5, MyHC) and pericytes markers (AP, PDGF-B RGS5 and NG2) of Dll4 and PDGF-BB treated embryonic and fetal Myf5^{GFP+} positive myoblasts compared to embryonic Pax3$^{GFP/+}$ positive myoblasts.

Data are expressed as mean ± SEM. *p < 0.05, **p < 0.005, ***p < 0.0005, ****p < 0.00005, ns: not significant one-way ANOVA. Scale bars, 50 μm.

absence of the coactivator MEF2 prevents myogenin transcriptional activation, thus blocking myogenesis (Figure 7H).

DISCUSSION

Pericytes are still poorly defined cells that express a number of markers, none of which is unique, and, moreover, not all markers are expressed simultaneously in the same cell, making their identification in vivo and their prospective isolation a difficult task (Armulik et al., 2011). Also, their origin is complex because they may derive from neural crest, paraxial, and lateral mesoderm (Díaz-Flores et al., 2009). They are recruited by endothelial cells through a PDGF-BB/PDGF-Rβ loop but can also derive from proliferation of pre-existing pericytes and, moreover, from endothelial-to-mesenchymal transition (Endo-MT) (DeRuiter et al., 1997; Zeisberg et al., 2007).

In contrast, myogenic cells have been thoroughly characterized and are unequivocally identified by the expression of a number of unique (MyoD, Myf5, MRF4) or restricted (Pax3, Pax7) transcription factors (Rudnicki et al., 2008). In contrast, their surface markers are often shared with other cell types and many, intriguingly, with pericytes. Notch and its ligands

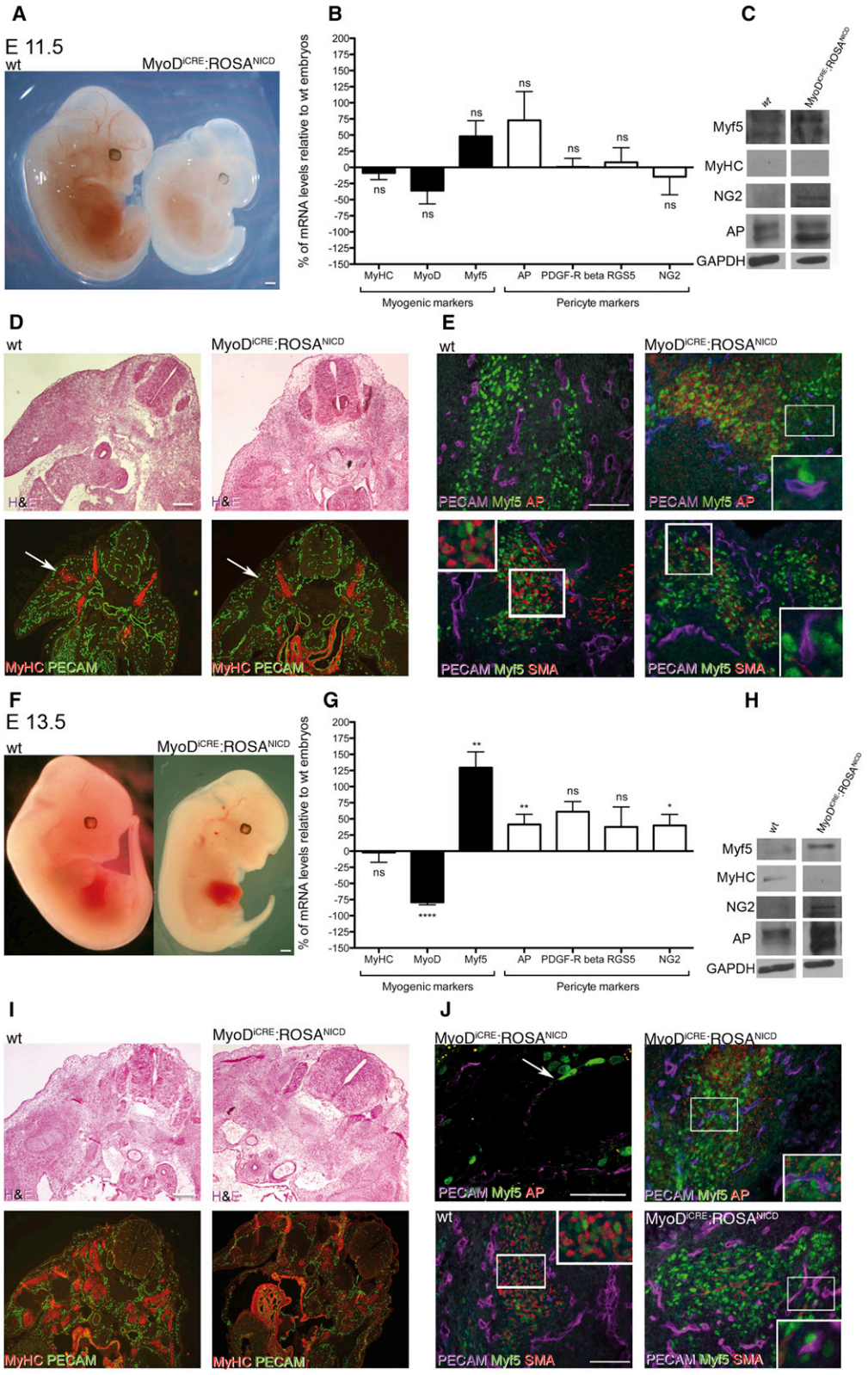

Figure 4. Analysis of Mutant and Control Embryos: E11.5 and E13.5

(A) Morphology of WT embryos compared to MyoD^{iCRE}:ROSA^{NICD} embryos at E11.5.

(B) Quantitative real-time PCR analysis of the expression of myogenic and pericyte markers of MyoD^{iCRE}:ROSA^{NICD} compared to WT embryos. Values are plotted as percentage (%) of control. Data are represented as mean ± SEM. ns, not significant. Unpaired t test.

(legend continued on next page)

play multiple roles in tissue development and regeneration (Andersson et al., 2011; Dahlqvist et al., 2003). In the case of growing blood vessels, Dll4 and PDGF-BB expressed by tip cells, respectively, bind Notch and PDGF-Rβ on surrounding mesoderm cells in order to regulate vessel growth and maturation (Hellström et al., 1999). In developing skeletal muscle, mesoderm tissue contains many skeletal myoblasts at different stages of proliferation, commitment, and differentiation, intimately associated with the growing vessel that in the adult will form a fine capillary network around each muscle fiber.

In this work, we show that already-committed skeletal myoblasts, if exposed to recruiting signals from the endothelium, can change their fate and enter the pericyte lineage. Indeed, whereas embryonic myoblasts are insensitive to most mitogens (Biressi et al., 2007b), they are inhibited only by Notch ligands. Interestingly, all the Notch ligands tested (Dll1, Dll4, and Jagged1) are able to suppress expression of myogenic genes (with the notable exception of Myf5). However, only Dll4 activates pericyte genes in committed $Pax3^+$ myoblasts and also in Myf5 or MyoD-expressing myoblasts, although with a slightly different pattern. Moreover, myogenic cells exposed in vitro to Dll4 and PDGF-BB adopted a perithelial position stabilizing vessel-like networks of endothelial cells both in vitro and in vivo, whether the untreated cells are not able to stabilize and endothelial network. Silencing of Dll4 in HUVECs blocks this effect thus providing evidence that also this ligand is required for pericyte recruitment, at least under these experimental conditions. Finally, if NICD is activated during embryonic development exclusively in MyoD-expressing cells, these cells downregulate myogenic gene expression, again with the exception of Myf5, and activate genes encoding for pericyte markers. Additionally, whenever myoblasts are located close to a vessel, they adopt a perithelial position while still maintaining a strong Myf5 expression. Under these experimental conditions, we observed the activation of a "pericyte fate" in most myogenic cells. This event is infrequent but not extremely rare also during normal embryogenesis, where both Myf5 and MyoD-expressing cells can be found associated to the vessel wall. Thus, it appears that endothelial cells can convert myogenic cells to pericytes, likely through Dll4 and PDGF-BB. These molecules likely act on cells in closest proximity to growing vessels. This also could explain why in mutant embryos, only a fraction of the $Myf5^+/AP^+$ cells adopt a perithelial position.

Of the two molecules involved, Dll4 appears to be the main actor because it can activate AP in vitro in the absence of PDGF-BB and because in the in vivo experiments, the endogenous levels of PDGF-BB were not altered. On the other hand, PDGF-BB is known to stimulate myoblast proliferation (Yablonka-Reuveni et al., 1990) and also recruitment of mesoderm cells by the endothelium (Hirschi et al., 1998), consistent with its ability to enhance Dll4 effect but not to replace it. At the molecular level, Dll4 and PDGF-BB activate different intracellular pathways that likely result in a cooperative effect on the resulting "pericyte" phenotype. Interestingly, it was reported that Notch activation leads to increased PDGF-Rβ in smooth muscle cells (Jin et al., 2008), similar to what we observe in skeletal myoblasts, and this may represent a mechanism reinforcing the action of Dll4 in this myoblast to pericyte conversion.

The fact that myogenic identity is not erased is in agreement with a recent report showing that activation of Notch in embryonic cells expressing Myf5 blocks myogenesis but not the developmental progression of the various myogenic populations (Mourikis et al., 2012). In our case, we observed that, in vitro, γ-secretase inhibition restores terminal myogenic differentiation; moreover, Myf5 continues to be expressed in vitro and in vivo at higher levels than WT, even though it fails to drive terminal differentiation. Notch downstream effectors Hairy and Hes1 are known to activate myogenic bHLH inhibitors such as Twist and Id (Tapanes-Castillo and Baylies, 2004; Reynaud-Deonauth et al., 2002). We confirm here that these genes are indeed upregulated in myogenic cells exposed to Dll4. Among these, Id3, the most strongly upregulated, sequesters Myf5, likely reducing its ability to bind the myogenin promoter, which still occurs but is ineffective owing to simultaneous inhibition of MEF2 expression (Gagan et al., 2012; Wilson-Rawls et al., 1999).

We recently showed that differentiating myofibers are able to recruit pericytes to a myogenic fate in vitro (Ugarte et al., 2012), in vivo (Dellavalle et al., 2011), and upon transplantation (Dellavalle et al., 2007; reviewed in Tedesco and Cossu, 2012), supporting the possibility of lineage promiscuity in solid mesoderm development. In addition, endothelial, smooth, and

(C) Western blot analysis of myogenic (Myf5, MyHC) and pericyte (NG2, AP) markers expressed by WT and $MyoD^{iCRE}$:$ROSA^{NICD}$ embryos at E11.5. Samples are shown as individual bands here and in Figure 5 because protein extracts from WT and mutant embryos were run on distinct gels even though the amount of proteins loaded (30 μg) was the same.
(D) H&E on transversal sections of WT and $MyoD^{iCRE}$:$ROSA^{NICD}$ embryos (upper panel); immunofluorescence analysis of serial transversal sections of the same embryos, stained with anti-MyHC (red) and anti-PECAM (green) antibodies. Scale bars, 50 μm.
(E) Immunofluorescence analysis of serial transversal sections of hindlimb of the embryos stained in (D) with anti-Myf5 (green) antibody, AP reaction (red) and anti-PECAM (violet) antibodies in the upper part of the panel; in the lower part, sections are stained with anti-Myf5 (green), anti-SMA (red), and anti-PECAM (violet) antibodies. Inset shows higher magnification of the area defined by the rectangle. Scale bars, 100 μm.
(F) Morphology of $MyoD^{iCRE}$:$ROSA^{NICD}$ mice and WT embryos at E13.5.
(G) Quantitative real-time PCR analysis of relative mRNA expression of myogenic (i.e., MyoD, Myf5, MyHC, and myogenin) and pericyte markers (i.e., NG2, RGS5, AP, PDGF-R) in WT and $MyoD^{iCRE}$:$ROSA^{NICD}$. Data are presented as mean ± SEM. *$p < 0.05$, **$p < 0.005$, ****$p < 0.00005$, unpaired t test.
(H) Western blot analysis of myogenic (Myf5, MyHC) and pericyte (NG2, AP) markers expressed by WT and $MyoD^{iCRE}$:$ROSA^{NICD}$ embryos at E13.5.
(I) H&E on transversal sections of $MyoD^{iCRE}$:$ROSA^{NICD}$ embryos at E13.5 (upper panel); immunofluorescence analysis of serial transversal section of the same embryos, stained with anti-MyHC (red) and anti-PECAM (green) antibodies, respectively, on WT and $MyoD^{iCRE}$:$ROSA^{NICD}$. Scale bars, 50 μm.
(J) Immunofluorescence analysis of serial transverse sections of hindlimb of embryos (I) stained with anti-Myf5 (green) antibody, AP reaction (red), and PECAM (violet) antibodies in the upper part of the panel; in the lower part, sections are stained with anti-Myf5 (green), anti-SMA (red), and anti-PECAM (violet) antibodies. Inset shows higher magnification of the area defined by the rectangle. Scale bars, 50 μm.
See also Figures S6 and S7.

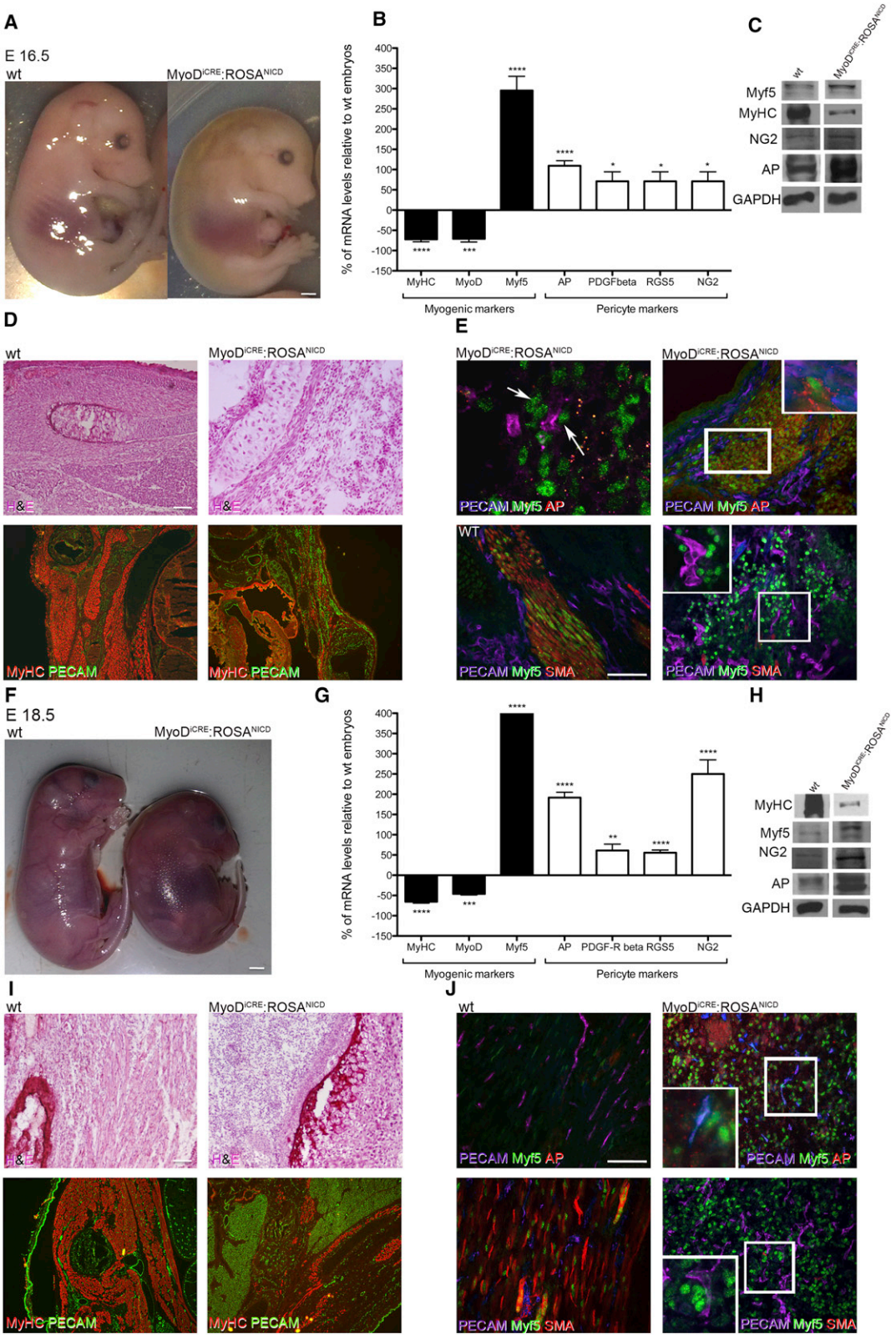

Figure 5. Analysis of Mutant and Control Fetus: E16.5 and E18.5

(A) Morphology of MyoD^{iCRE}:ROSA^{NICD} and WT fetuses at E16.5.

(B) Quantitative real-time PCR analysis of relative mRNA analysis of MyoD, Myf5, MyHC, and myogenin and of NG2, RGS5, AP, and PDGF in WT and MyoD^{iCRE}:ROSA^{NICD} fetuses. Data are represented as mean ± SEM. *p < 0.05, **p < 0.005, ****p < 0.00005, unpaired t test.

(legend continued on next page)

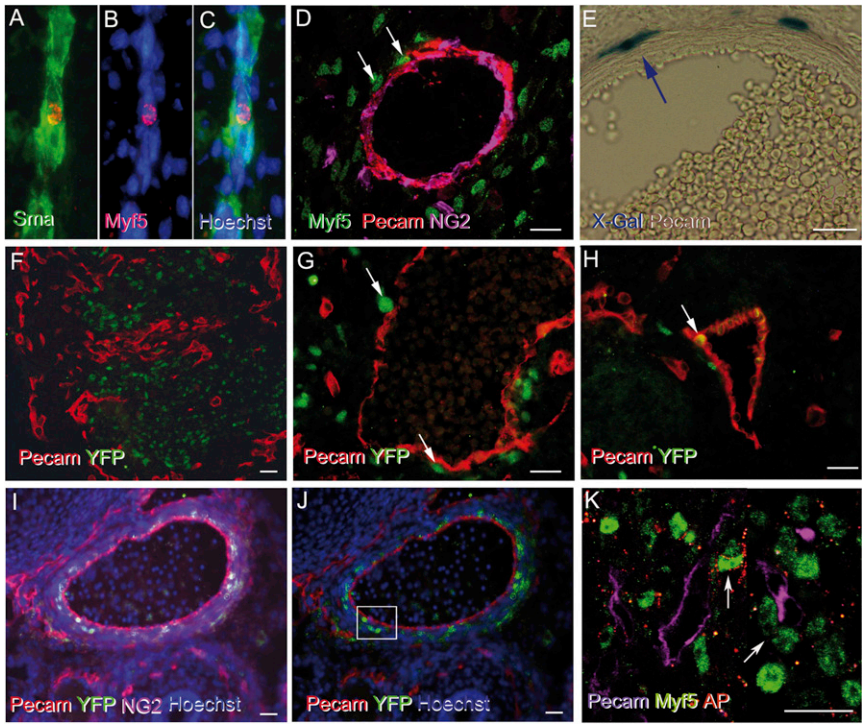

Figure 6. Immunofluorescence Analysis of Myogenic and Pericyte Markers in Normal Embryos

(A–C) Immunofluorescence analysis with anti-SMA (green, A) or anti-Myf5 (red, B) antibodies of a vessel in an E16.5 WT fetus. Nuclei are stained with Hoechst (blue). Merged image in (C).

(D) Immunofluorescence analysis of the same fetus, showing a transverse section of a medium-size vessel, stained with anti-Myf5 (green), anti-NG2 (violet), and anti-PECAM (red) antibodies. Arrows indicate two Myf5$^+$ cells closely associated with the vessel muscular layer.

(E) X-Gal staining of a transverse section of a vessel from a phenotypically normal MyoD^{iCRE}:ROSA^{NZG} fetus at E16.5. Two nuclear LacZ-positive cells, derived from MyoD-expressing cell(s), are found in a perithelial position, showing a typical pericyte nucleus (arrow).

(F–H) Immunofluorescence analysis of a transversal section from MyoD^{iCRE}:ROSA^{EYFP} fetus at E16.5, stained with anti-PECAM (red) and anti-GFP (green) antibodies, showing normal intermixing of myoblasts and endothelial cells in (F). In (G) and (H), several YFP$^+$ nuclei, hence, derived from MyoD-expressing cells, are detected closely associated with the vessel wall (arrows).

(I and J) Immunofluorescence of a transversal section from MyoD^{iCRE}:ROSA^{EYFP} at E16.5, stained with anti-PECAM (red), anti-GFP (green), anti-NG2 (violet), and Hoechst (blue) reveals several YFP$^+$ cells associated to the vessel wall (J). The same image is shown without the NG2 channel to more clearly reveal YFP$^+$ cells. Inset shows three eYFP$^+$ cells adjacent to the endothelium (PECAM$^+$). Rectangle shows the colabeling with NG2 and eYFP.

(K) Confocal immunofluorescence of a transverse section from E16.5 WT fetus, stained with anti-PECAM (violet), anti-Myf5 (green) antibodies and AP (red) reaction. Arrows show AP$^+$, Myf5$^+$ cells adjacent to the endothelium.

Scale bars, 100 μm. See also Figure S7.

skeletal muscle progenitors originate in the dermomyotome where fate choice is dictated by signaling molecules such as BMP, TGF-β, and Notch (Ben-Yair and Kalcheim, 2008). Indeed, Pax3-expressing myogenic precursors are also able to migrate ventrally and contribute to the smooth muscle of the aorta (Esner et al., 2006; Lagha et al., 2009).

We now show that specific signaling molecules act also at later stages of development and are therefore able to drive conversion (i.e., fate change from skeletal to smooth muscle) in already-committed cells. Hence, it appears that during embryogenesis, cells adopt a specific fate depending upon the timely and appropriate exposure to signaling molecules emanating from the surrounding cells (Bonfanti et al., 2012). However, these fate choices are not irreversibly fixed but are reinforced and stabilized by the microenvironment (Bonfanti et al., 2010; Booth et al., 2008). In the case of developing skeletal muscle,

(C) Western blot analysis of myogenic (Myf5, MyHC) and pericyte (NG2, AP) markers expressed by WT and MyoD^{iCRE}:ROSA^{NICD} fetuses.

(D) H&E of longitudinal sections of fetal limbs (upper panel); immunofluorescence analysis of transversal sections of the trunk of the same fetus, stained with anti-MyHC (red) and anti-PECAM (green) antibodies. Scale bar, 50 μm.

(E) Immunofluorescence of serial transversal sections of MyoD^{iCRE}:ROSA^{NICD} hindlimb stained with anti-Myf5 (green) antibody, AP reaction (red), and anti-PECAM (violet) antibody in two different magnifications. Left upper part of the panel shows confocal analysis; in the lower part of the panel, sections are stained with anti-Myf5 (green), anti-SMA (red), and anti-PECAM (violet) antibodies. Left image depicts WT fetus, whereas the right shows a MyoD^{iCRE}:ROSA^{NICD} one. Inset shows higher magnification of the area defined by the rectangle. Scale bar, 100 μm.

(F) Morphology of MyoD^{iCRE}:ROSA^{NICD} mice and WT fetuses at E18.5.

(G) Quantitative real-time PCR analysis of relative mRNA analysis of MyoD, MyHC, myogenin, NG2, RGS5, AP and PDGFB in WT and MyoD^{iCRE}:ROSA^{NICD} fetuses. Data are represented as mean ± SEM. **$p < 0.05$, ***$p < 0.005$, ****$p < 0.00005$, unpaired t test.

(H) Western blot analysis of myogenic (Myf5, MyHC) and pericyte (NG2, AP) markers expressed by WT fetuses and MyoD^{iCRE}:ROSA^{NICD} fetuses. Immunofluorescence of serial transversal sections of trunk stained with anti-MyHC (red) and anti-PECAM (green) antibodies. Scale bars, 50 μm.

(I) H&E of longitudinal sections of fetal limbs (upper panel); immunofluorescence analysis of transversal sections of the trunk of the same fetus, stained with anti-MyHC (red) and anti-PECAM (green) antibodies. Scale bar, 50 μm.

(J) Immunofluorescence of serial transversal sections of hindlimb stained with anti-Myf5 (green) and anti-PECAM (violet) antibodies and AP (red) reaction. In the upper part of the panel of both WT (left) and MyoD^{iCRE}:ROSA^{NICD} (right) fetuses; in the lower part of the panel, sections of both WT (left) and MyoD^{iCRE}:ROSA^{NICD} (right) fetuses are stained with anti-antibodies against Myf5 (green), anti-SMA (red), and anti-PECAM (violet) antibodies. Inset shows higher magnification of the area defined by the rectangle. Scale bar, 100 μm.

See also Figures S6 and S7.

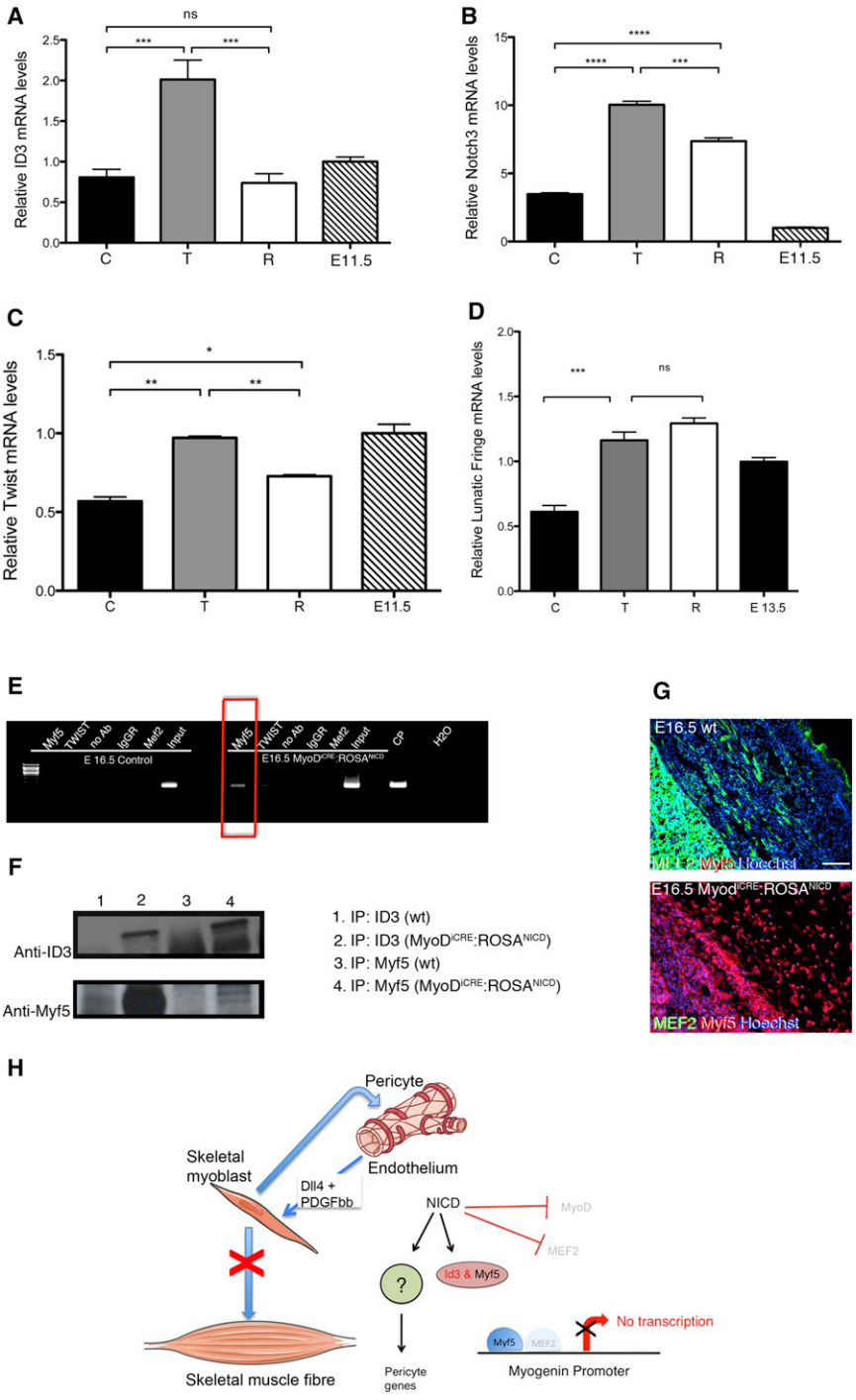

Figure 7. Notch Target Gene Activation Prevents Myf5-Mediated Myogenesis by Both Sequestering Myf5 and Inhibiting MEF2 Expression

(A–D) Quantitative real-time PCR analysis of ID3 (A), Notch3 (B), Twist (C), and Lunatic Fringe (D): relative mRNA level of control (C), Dll4 and PDGF-BB treated (T), and reverted (L-685,458) (R). Pax3$^{GFP/+}$ cells from E11.5 embryos. Data are represented as mean ± SEM. *p < 0.05, ***p < 0.005 **p < 0.005, ****p < 0.00005, one-way ANOVA.

(E) ChIP analysis of WT and MyoD^{iCRE}:ROSA^{NICD} fetuses at E16.5 showing binding of Myf5 on the myogenin promoter only in mutant fetus.

(F) Immunoprecipitation of WT and MyoD^{iCRE}:ROSA^{NICD} fetuses at E16.5, revealing binding between ID3 and Myf5.

(G) Double-immunofluorescence analysis of limbs at E16.5, stained with anti-MEF2 (green) and anti-Myf5 antibodies. WT fetuses stained with anti-MCF2 (green) and anti Myf5 (red) antibodies. Bone on the left shows nonspecific background staining. Scale bar, 50 μm.

(H) A model proposing a molecular mechanism regulating the conversion of myogenic progenitors to a pericyte fate.

developing fibers and endothelium may compete for surrounding mesoderm cells, whose final fate is irreversibly fixed only at the onset of terminal differentiation.

EXPERIMENTAL PROCEDURES

Mutant Animals and Genotyping

The Pax3$^{GFP/+}$ (Relaix et al., 2005), MyoD^{iCRE} (Kanisicak et al., 2009), and ROSA^{NICD} (Murtaugh et al., 2003) mice were genotyped as previously described. All experiments were performed following regulations for animal care and handlings (San Raffaele Hospital IACUC 355; UK Home Office Project License PPL no. 70/7435).

Cell Isolation and Cell Culture

Cell isolation and cell cultures are detailed in the Supplemental Experimental Procedures. Briefly, embryonic myoblasts were obtained from dissection of somites and limbs of E11.5 Pax3$^{GFP/+}$embryos. Tissues were enzymatically dissociated for 20 min. Dissociated cells were suspended in DMEM-high glucose (GIBCO), supplemented with 20% horse serum (HS; BioWhittaker), 20 mM HEPES, and 2 mM EDTA (Sigma-Aldrich) and filtered before sorting. NG2^{+}/PECAM^{-}-positive cells were isolated from the GFP-negative counterpart of Pax3$^{GFP/+}$ embryos or Homo-GFP (Hadjantonakis et al., 1998) mouse thus avoiding contamination of myogenic cells.

For skeletal muscle differentiation, Pax3$^{GFP/+}$-sorted embryonic myoblasts were suspended in DMEM-high glucose supplemented with 20% HS onto collagen-coated dishes. Alternatively, embryonic myoblasts were plated onto Dll4 (R&D Systems; 1389-D4) 10 μg/ml-coated dishes and grown in DMEM-high glucose medium supplemented with 20% HS and PDGF-BB (Sigma-Aldrich) at a concentration of 50 μg/ml. HUVECs were cultured in MCDB 131 (GIBCO) medium with endothelial cell supplements as described previously (Lampugnani et al., 2002). 10T$^{1/2}$ fibroblasts were cultured in DMEM-high glucose supplemented with 10% fetal calf serum on collagen-coated dishes.

Endothelial Cell Transfection

HUVECs were transfected at passage 1 using Lipofectamine (LTX&PLUS reagent), with four different shRNAs targeting Dll4 (#1, #2, #3, and #4,

GeneCopoeia HSH013577) and with a scramble shRNA as a control for specificity. Briefly, 1.5×10^5 cells were plated into a 24-well. A total of 0.5 μg of DNA was diluted into Opti-MEM and added to the cells according to the manufacturer's instructions. Cells were then incubated for 18–24 hr and then analyzed under a fluorescence microscope. qPCR analysis of Dll4 expression was performed to select the best shRNA, and Matrigel plug assay was performed with HUVECs after Dll4 silencing.

Angiogenic and Matrigel Plug Assays

Angiogenic assays were performed as already described in Akhtar et al. (2002). Additional details are available in the Supplemental Experimental Procedures. For Matrigel plug assay, HUVECs (4×10^6 cells/ml) were mixed with $Pax3^{GFP/+}$ (5×10^5 cells), either untreated or previously treated with Dll4 and PDGF-BB. Five hundred microliters of Matrigel-reduced growth factor (BD; Matrigel 356230) was mixed at a ratio of 1:1 with the cell suspension (containing both HUVECs and either treated or untreated $Pax3^{GFP/+}$ cells) and promptly injected subcutaneously in the dorsal region of 2.5- to 3.5-month-old nude mice. Plugs were recovered after 2–4 weeks after implant and then embedded in OCT, cryostat sectioned, and processed for immunofluorescence analysis.

ChIP Assay and Immunoprecipitation

The ChIP protocol was performed on fetuses (E16.5) as previously described (Messina et al., 2010). The following antibodies were used: rabbit anti-MEF2 (C21 sc-313X, 200 mg/0.1 ml; Santa Cruz Biotechnology); rabbit anti-Myf5 (Sc-302; Santa Cruz Biotechnology); and, as a control, normal rabbit IgGr (Santa Cruz Biotechnology). Immunoprecipitated DNA was subjected to PCR as detailed in the Supplemental Experimental Procedures. A detailed description of the immunoprecipitation assay is available in the Supplemental Experimental Procedures.

AP, Immunofluorescence, and Western Blot Analyses

AP reaction, immunofluorescence, and western blot on cells and tissues were carried out as previously described in Tedesco et al. (2011) or detailed in Supplemental Experimental Procedures.

SUPPLEMENTAL INFORMATION

Supplemental Information includes seven figures and Supplemental Experimental Procedures and can be found with this article online at http://dx.doi.org/10.1016/j.devcel.2013.01.022.

ACKNOWLEDGMENTS

Work in the authors' laboratory is supported by grants from the European Community (OptiStem, Angioscaff, and Biodesign), MRC, ERC, Telethon, Duchenne Parent Project, and the Italian Ministries of Research and of Health. We thank S. Antonini for excellent technical help, A. Dellavalle and members of the laboratory for suggestions and discussion, and S. Boast and S. Price for revising the manuscript. We thank E. Dejana and S. Tajbakhsh for helpful discussions and antibodies. We also thank D. Goldhammer, F. Radtke, and D. Melton for providing mice.

Received: May 3, 2012
Revised: December 21, 2012
Accepted: January 28, 2013
Published: March 7, 2013

REFERENCES

Akhtar, N., Dickerson, E.B., and Auerbach, R. (2002). The sponge/Matrigel angiogenesis assay. Angiogenesis *5*, 75–80.

Andersson, E.R., Sandberg, R., and Lendahl, U. (2011). Notch signaling: simplicity in design, versatility in function. Development *138*, 3593–3612.

Armulik, A., Genové, G., and Betsholtz, C. (2011). Pericytes: developmental, physiological, and pathological perspectives, problems, and promises. Dev. Cell *21*, 193–215.

Babai, F., Musevi-Aghdam, J., Schurch, W., Royal, A., and Gabbiani, G. (1990). Coexpression of alpha-sarcomeric actin, alpha-smooth muscle actin and desmin during myogenesis in rat and mouse embryos I. Skeletal muscle. Differentiation *44*, 132–142.

Ben-Yair, R., and Kalcheim, C. (2008). Notch and bone morphogenetic protein differentially act on dermomyotome cells to generate endothelium, smooth, and striated muscle. J. Cell Biol. *180*, 607–618.

Bianco, P., and Cossu, G. (1999). Uno, nessuno e centomila: searching for the identity of mesodermal progenitors. Exp. Cell Res. *251*, 257–263.

Biressi, S., Molinaro, M., and Cossu, G. (2007a). Cellular heterogeneity during vertebrate skeletal muscle development. Dev. Biol. *308*, 281–293.

Biressi, S., Tagliafico, E., Lamorte, G., Monteverde, S., Tenedini, E., Roncaglia, E., Ferrari, S., Ferrari, S., Cusella-De Angelis, M.G., Tajbakhsh, S., and Cossu, G. (2007b). Intrinsic phenotypic diversity of embryonic and fetal myoblasts is revealed by genome-wide gene expression analysis on purified cells. Dev. Biol. *304*, 633–651.

Bonfanti, P., Claudinot, S., Amici, A.W., Farley, A., Blackburn, C.C., and Barrandon, Y. (2010). Microenvironmental reprogramming of thymic epithelial cells to skin multipotent stem cells. Nature *466*, 978–982.

Bonfanti, P., Barrandon, Y., and Cossu, G. (2012). 'Hearts and bones': the ups and downs of 'plasticity' in stem cell biology. EMBO Mol. Med. *4*, 353–361.

Booth, B.W., Boulanger, C.A., and Smith, G.H. (2008). Stem cells and the mammary microenvironment. Breast Dis. *29*, 57–67.

Buckingham, M., and Relaix, F. (2007). The role of Pax genes in the development of tissues and organs: Pax3 and Pax7 regulate muscle progenitor cell functions. Annu. Rev. Cell Dev. Biol. *23*, 645–673.

Cossu, G., and Borello, U. (1999). Wnt signaling and the activation of myogenesis in mammals. EMBO J. *18*, 6867–6872.

Cossu, G., Kelly, R., Tajbakhsh, S., Di Donna, S., Vivarelli, E., and Buckingham, M. (1996). Activation of different myogenic pathways: myf-5 is induced by the neural tube and MyoD by the dorsal ectoderm in mouse paraxial mesoderm. Development *122*, 429–437.

Dahlqvist, C., Blokzijl, A., Chapman, G., Falk, A., Dannaeus, K., Ibáñez, C.F., and Lendahl, U. (2003). Functional Notch signaling is required for BMP4-induced inhibition of myogenic differentiation. Development *130*, 6089–6099.

Delfini, M.C., Hirsinger, E., Pourquié, O., and Duprez, D. (2000). Delta 1-activated notch inhibits muscle differentiation without affecting Myf5 and Pax3 expression in chick limb myogenesis. Development *127*, 5213–5224.

Dellavalle, A., Sampaolesi, M., Tonlorenzi, R., Tagliafico, E., Sacchetti, B., Perani, L., Innocenzi, A., Galvez, B.G., Messina, G., Morosetti, R., et al. (2007). Pericytes of human skeletal muscle are myogenic precursors distinct from satellite cells. Nat. Cell Biol. *9*, 255–267.

Dellavalle, A., Maroli, G., Covarello, D., Azzoni, E., Innocenzi, A., Perani, L., Antonini, S., Sambasivan, R., Brunelli, S., Tajbakhsh, S., et al. (2011). Pericytes resident in postnatal skeletal muscle differentiate into muscle fibres and generate satellite cells. Nat. Commun. *2*, 499.

DeRuiter, M.C., Poelmann, R.E., VanMunsteren, J.C., Mironov, V., Markwald, R.R., and Gittenberger-de Groot, A.C. (1997). Embryonic endothelial cells transdifferentiate into mesenchymal cells expressing smooth muscle actins in vivo and in vitro. Circ. Res. *80*, 444–451.

De Strooper, B., Annaert, W., Cupers, P., Saftig, P., Craessaerts, K., Mumm, J.S., Schroeter, E.H., Schrijvers, V., Wolfe, M.S., Ray, W.J., et al. (1999). A presenilin-1-dependent gamma-secretase-like protease mediates release of Notch intracellular domain. Nature *398*, 518–522.

Díaz-Flores, L., Gutiérrez, R., Madrid, J.F., Varela, H., Valladares, F., Acosta, E., Martín-Vasallo, P., and Díaz-Flores, L., Jr. (2009). Pericytes. Morphofunction, interactions and pathology in a quiescent and activated mesenchymal cell niche. Histol. Histopathol. *24*, 909–969.

Esner, M., Meilhac, S.M., Relaix, F., Nicolas, J.F., Cossu, G., and Buckingham, M.E. (2006). Smooth muscle of the dorsal aorta shares a common clonal origin with skeletal muscle of the myotome. Development *133*, 737–749.

Gagan, J., Dey, B.K., Layer, R., Yan, Z., and Dutta, A. (2012). Notch3 and Mef2c proteins are mutually antagonistic via Mkp1 protein and miR-1/206 microRNAs in differentiating myoblasts. J. Biol. Chem. *287*, 40360–40370.

Hadjantonakis, A.K., Gertsenstein, M., Ikawa, M., Okabe, M., and Nagy, A. (1998). Generating green fluorescent mice by germline transmission of green fluorescent ES cells. Mech. Dev. *76*, 79–90.

Hellström, M., Kalén, M., Lindahl, P., Abramsson, A., and Betsholtz, C. (1999). Role of PDGF-B and PDGFR-beta in recruitment of vascular smooth muscle cells and pericytes during embryonic blood vessel formation in the mouse. Development *126*, 3047–3055.

Herman, I.M., and D'Amore, P.A. (1985). Microvascular pericytes contain muscle and nonmuscle actins. J. Cell Biol. *101*, 43–52.

Hirschi, K.K., Rohovsky, S.A., and D'Amore, P.A. (1998). PDGF, TGF-beta, and heterotypic cell-cell interactions mediate endothelial cell-induced recruitment of 10T1/2 cells and their differentiation to a smooth muscle fate. J. Cell Biol. *141*, 805–814.

Jin, S., Hansson, E.M., Tikka, S., Lanner, F., Sahlgren, C., Farnebo, F., Baumann, M., Kalimo, H., and Lendahl, U. (2008). Notch signaling regulates platelet-derived growth factor receptor-beta expression in vascular smooth muscle cells. Circ. Res. *102*, 1483–1491.

Kanisicak, O., Mendez, J.J., Yamamoto, S., Yamamoto, M., and Goldhamer, D.J. (2009). Progenitors of skeletal muscle satellite cells express the muscle determination gene, MyoD. Dev. Biol. *332*, 131–141.

Kopan, R., Nye, J.S., and Weintraub, H. (1994). The intracellular domain of mouse Notch: a constitutively activated repressor of myogenesis directed at the basic helix-loop-helix region of MyoD. Development *120*, 2385–2396.

Kume, T. (2012). Ligand-dependent Notch signaling in vascular formation. Adv. Exp. Med. Biol. *727*, 210–222.

Lagha, M., Brunelli, S., Messina, G., Cumano, A., Kume, T., Relaix, F., and Buckingham, M.E. (2009). Pax3:Foxc2 reciprocal repression in the somite modulates muscular versus vascular cell fate choice in multipotent progenitors. Dev. Cell *17*, 892–899.

Lampugnani, M.G., Zanetti, A., Breviario, F., Balconi, G., Orsenigo, F., Corada, M., Spagnuolo, R., Betson, M., Braga, V., and Dejana, E. (2002). VE-cadherin regulates endothelial actin activating Rac and increasing membrane association of Tiam. Mol. Biol. Cell *13*, 1175–1189.

Langlands, K., Yin, X., Anand, G., and Prochownik, E.V. (1997). Differential interactions of Id proteins with basic-helix-loop-helix transcription factors. J. Biol. Chem. *272*, 19785–19793.

Messina, G., Biressi, S., Monteverde, S., Magli, A., Cassano, M., Perani, L., Roncaglia, E., Tagliafico, E., Starnes, L., Campbell, C.E., et al. (2010). Nfix regulates fetal-specific transcription in developing skeletal muscle. Cell *140*, 554–566.

Mourikis, P., Gopalakrishnan, S., Sambasivan, R., and Tajbakhsh, S. (2012). Cell-autonomous Notch activity maintains the temporal specification potential of skeletal muscle stem cells. Development *139*, 4536–4548.

Murtaugh, L.C., Stanger, B.Z., Kwan, K.M., and Melton, D.A. (2003). Notch signaling controls multiple steps of pancreatic differentiation. Proc. Natl. Acad. Sci. USA *100*, 14920–14925.

Nakatsu, M.N., Sainson, R.C., Aoto, J.N., Taylor, K.L., Aitkenhead, M., Pérez-del-Pulgar, S., Carpenter, P.M., and Hughes, C.C. (2003). Angiogenic sprouting and capillary lumen formation modeled by human umbilical vein endothelial cells (HUVEC) in fibrin gels: the role of fibroblast and Angiopoietin-1. Microvasc. Res. *66*, 102–112.

Ott, M.O., Bober, E., Lyons, G., Arnold, H., and Buckingham, M. (1991). Early expression of the myogenic regulatory gene, myf-5, in precursor cells of skeletal muscle in the mouse embryo. Development *111*, 1097–1107.

Relaix, F., Rocancourt, D., Mansouri, A., and Buckingham, M. (2005). A Pax3/Pax7-dependent population of skeletal muscle progenitor cells. Nature *435*, 948–953.

Reynaud-Deonauth, S., Zhang, H., Afouda, A., Taillefert, S., Beatus, P., Kloc, M., Etkin, L.D., Fischer-Lougheed, J., and Spohr, G. (2002). Notch signaling is involved in the regulation of Id3 gene transcription during *Xenopus* embryogenesis. Differentiation *69*, 198–208.

Rudnicki, M.A., Schnegelsberg, P.N., Stead, R.H., Braun, T., Arnold, H.H., and Jaenisch, R. (1993). MyoD or Myf-5 is required for the formation of skeletal muscle. Cell *75*, 1351–1359.

Rudnicki, M.A., Le Grand, F., McKinnell, I., and Kuang, S. (2008). The molecular regulation of muscle stem cell function. Cold Spring Harb. Symp. Quant. Biol. *73*, 323–331.

Scehnet, J.S., Jiang, W., Kumar, S.R., Krasnoperov, V., Trindade, A., Benedito, R., Djokovic, D., Borges, C., Ley, E.J., Duarte, A., and Gill, P.S. (2007). Inhibition of Dll4-mediated signaling induces proliferation of immature vessels and results in poor tissue perfusion. Blood *109*, 4753–4760.

Schuster-Gossler, K., Cordes, R., and Gossler, A. (2007). Premature myogenic differentiation and depletion of progenitor cells cause severe muscle hypotrophy in Delta1 mutants. Proc. Natl. Acad. Sci. USA *104*, 537–542.

Tapanes-Castillo, A., and Baylies, M.K. (2004). Notch signaling patterns Drosophila mesodermal segments by regulating the bHLH transcription factor twist. Development *131*, 2359–2372.

Tedesco, F.S., and Cossu, G. (2012). Stem cell therapies for muscle disorders. Curr. Opin. Neurol. *25*, 597–603.

Tedesco, F.S., Hoshiya, H., D'Antona, G., Gerli, M.F., Messina, G., Antonini, S., Tonlorenzi, R., Benedetti, S., Berghella, L., Torrente, Y., et al. (2011). Stem cell-mediated transfer of a human artificial chromosome ameliorates muscular dystrophy. Sci. Transl. Med. *3*, 96ra78.

Ugarte, G., Cappellari, O., Perani, L., Pistocchi, A., and Cossu, G. (2012). Noggin recruits mesoderm progenitors from the dorsal aorta to a skeletal myogenic fate. Dev. Biol. *365*, 91–100.

Wilson-Rawls, J., Molkentin, J.D., Black, B.L., and Olson, E.N. (1999). Activated notch inhibits myogenic activity of the MADS-Box transcription factor myocyte enhancer factor 2C. Mol. Cell. Biol. *19*, 2853–2862.

Yablonka-Reuveni, Z., Balestreri, T.M., and Bowen-Pope, D.F. (1990). Regulation of proliferation and differentiation of myoblasts derived from adult mouse skeletal muscle by specific isoforms of PDGF. J. Cell Biol. *111*, 1623–1629.

Zeisberg, E.M., Potenta, S., Xie, L., Zeisberg, M., and Kalluri, R. (2007). Discovery of endothelial to mesenchymal transition as a source for carcinoma-associated fibroblasts. Cancer Res. *67*, 10123–10128.